Micromechanical Analysis of the Binding of DNA-Bending Proteins HMGB1, NHP6A, and HU Reveals Their Ability To Form Highly Stable DNA−Protein Complexes†

Dunja Skoko,‡,§ Ben Wong,||,⊥ Reid C. Johnson,||,# and John F. Marko*,‡

Department of Physics, University of Illinois at Chicago, Chicago, Illinois 60607-7059, and Department of Biological Chemistry, David Geffen School of Medicine at UCLA, Los Angeles, California 90095-1737

Received July 22, 2004; Revised Manuscript Received August 17, 2004

ABSTRACT: The mechanical response generated by binding of the nonspecific DNA-bending proteins HMGB1, NHP6A, and HU to single tethered 48.5 kb λ-DNA molecules is investigated using DNA micromanipulation. As protein concentration is increased, the force needed to extend the DNA molecule increases, due to its compaction by protein-generated bending. Most significantly, we find that for each of HMGB1, NHP6A, and HU there is a well-defined protein concentration, not far above the binding threshold, above which the proteins do not spontaneously dissociate. In this regime, the amount of protein bound to the DNA, as assayed by the degree to which the DNA is compacted, is unperturbed either by replacing the surrounding protein solution with protein-free buffer or by straightening of the molecule by applied force. Thus, the stability of the protein−DNA complexes formed is dependent on the protein concentration during the binding. HU is distinguished by a switch to a DNA-stiffening function at the protein concentration where the formation of highly stable complexes occurs. Finally, introduction of competitor DNA fragments into the surrounding solution disassembles the stable DNA complexes with HMGB1, NHP6A, and HU within seconds. Since spontaneous dissociation of protein does not occur on a time scale of hours, we conclude that this rapid protein exchange in the presence of competitor DNA must occur only via "direct" DNA−DNA contact. We therefore observe that protein transport along DNA by direct transfers occurs even for proteins such as NHP6A and HU that have only one DNA-binding domain.

Non-histone DNA-bending proteins are associated with chromosomes of prokaryotic and eukaryotic cells. Prominent among these in eukaryotes are the nonspecifically binding class of HMGB[1] proteins, present in the nucleus at micromolar concentrations (*1*−*3*). HMGB proteins possess a ∼75 amino acid residue DNA-minor-groove-binding domain, which induces a bend of about 90°. Charged residues within extended peptide segments at the N- or C-termini of the HMGB domain can strongly modulate DNA binding affinities of these proteins. *Saccharomyces cerevisiae* NHP6A contains one HMGB domain but binds DNA with considerably higher affinity than mammalian HMGB1, which contains two domains (*4*). HMGB proteins function in a variety of localized DNA transactions including assembly of transcription and recombination complexes and chromatin remodeling (*1*−*3*). A general role for HMGB proteins in modulating global DNA organization in eukaryotes is not yet established, but yeast HMGB proteins have been shown to condense chromosomal DNA in prokaryotic models (*4*, *5*).

HU is the most abundant nonspecifically binding protein in the nucleoid of all prokaryotes and some organelles in eukaryotes (*6*−*9*). The structure of the HU dimer is unrelated to the HMGB fold, but it also associates with the DNA minor groove and induces flexible bends into DNA (*10*−*14*). Measurements of DNA bend angles generated by HU dimers range from roughly 70° (*11*, *13*) to as large as 140° for DNAs containing unpaired bases (*12*). The variability of bend angle suggests that the HU−DNA complex is able to accommodate a range of DNA bending (*14*). HU's DNA-bending activity is central to its role in a number of different reactions involving assembly of higher-order nucleoprotein complexes in bacteria; notably, HMGB proteins can substitute for HU in some of these reactions (*6*, *8*, *9*). HU mutant phenotypes have implicated HU as being a determinant in bacterial chromosome condensation (*4*, *15*−*17*).

In this report, we study binding and unbinding of HMGB1, NHP6A, and HU on large (48.5 kb) tethered λ-DNA molecules by following the mechanical response of the DNA

† This research was supported by the NSF through Grant DMR-0203963, by the Johnson and Johnson Focused Giving Program, and by the UIC Campus Research Board. B.W and R.C.J. were supported by USPHS Grant GM38501.

* Corresponding author. Tel: 312 996 6105. Fax: 312 996 9016. E-mail: jmarko@uic.edu.

‡ University of Illinois at Chicago.

§ Tel: 312 996 6105. Fax: 312 996 9106. E-mail: dskoko1@uic.edu.

|| David Geffen School of Medicine at UCLA.

⊥ Present address: Department of Biology, MIT, Cambridge, MA 02142. Tel: 617 253 4704. Fax: 617 253 8699. E-mail: bwong@mit.edu.

Tel: 310 825 7800. Fax: 310 206 5272. E-mail: rcjohnson@mednet.ucla.edu.

[1] Abbreviations: CCD, charge-coupled device; FRET, fluorescence resonance energy transfer; HMGB, high mobility group, class B; IHF, integration host factor; NA, numerical aperture; NHP6A, non-histone protein 6A; PAGE, polyacrylamide gel electrophoresis; PBS, phosphate-buffered saline; pN, piconewton; SFM, scanning force microscopy.

10.1021/bi048428o CCC: $27.50
Published on Web 10/05/2004

in real time (*18*, *19*). As these proteins bind and bend the DNA double helix, the force needed to extend the molecule is increased (*20*−*23*), allowing us to sensitively detect protein binding. In addition to detection of protein binding, our experiment permits us to directly observe and quantitatively measure how these proteins control DNA compaction, which is likely to be one of their functions in vivo. This approach is similar to that used by Ali et al. (*20*) to study IHF−DNA interactions.

HMGB1, NHP6A, and HU all equilibrate onto DNA within seconds, but subsequent dissociation kinetics into protein-free buffer are highly variable and reflect the protein concentration during binding. Our experiments show that formation of stable complexes occurs above specific protein concentrations, i.e., that the stability of the protein−DNA complexes depends on the protein concentration in solution during the binding process. Under all conditions, however, HMGB1−, NHP6A−, and HU−DNA complexes immediately disassemble when nonspecific DNA is present in solution. For HU, the onset of stabilization coincides with a switch from a DNA compaction to a DNA stiffening mode of binding. Our data support the qualitative picture discussed by Dame and Goosen on the basis of SFM visualization of HU−DNA complexes (*9*) and are in good quantitative accord with single-DNA experiments with HU reported very recently by van Noort et al. (*24*). The striking change of mechanical properties of long DNA molecules as a function of HU concentration helps to explain previously reported and sometimes conflicting properties of HU−DNA complexes in vitro (*9*).

EXPERIMENTAL PROCEDURES

Proteins and Binding Buffers. Native full-length HMGB1 was extracted from calf thymus and purified as described (*25*). Recombinant NHP6A was purified from *Escherichia coli* essentially as described (*26*), except that an additional FPLC mono S chromatography step was included. HU was purified from RJ5814 (*hip::cat fis::kan-767 endA*::Tn*10 his ilv λcI857 N*$^+$ containing pP_L-*hupAB* from R. McMacken) by a protocol involving chromatography on SP-Sepharose and mono S (Amersham Biosciences). All experiments used 20 mM HEPES−NaOH pH 7.5, 40 mM NaCl at 25 °C.

Flow Cell and DNA Tethering. Experiments were performed in flow cells of total volume 40 μL and of total thickness 1.2 mm, with a top surface made of #1 cover glass, with antidigoxygenin (Roche Diagnostics, Indianapolis, IN) covalently bound using standard methods (*27*). Linear 48502 bp λ-DNA (Promega, Madison, WI) was labeled at the left end with a biotin and at the right end with a digoxygenin by ligation of oligomers 5′-AGGTCGCCGCCC-biotin and 5′-GGGCGGCGACCT-digoxygenin (Proligo, San Diego CA). The DNA was incubated with streptavidin-coated paramagnetic beads (M-280, Dynal, Lake Success, NY) in phosphate-buffered saline (BioWhitaker, Walkersville, MD). The resulting bead−DNA structures were then injected into the flow cell, allowing binding of the digoxygenin-labeled DNA to the antibody-functionalized cover glass (*19*).

Microscope and Magnetic Tweezer. Beads near the cover glass were observed using a 100 × 1.35 NA oil objective (UplanApo, Olympus, Melville, NY), mounted on a piezoelectric translator (Mipos-3, PiezoJena, Jena, Germany), allowing 100 μm motion in 25 nm steps. The high NA gives a narrow depth of field, which is important for tracking the *z*-position of the beads. Illumination was done via the objective using a beam-splitter (see Figure 1); a lens formed an image on a CCD camera (HomeConnect, 3Com, Santa Clara, CA). Two cylindrical NdFeB magnets (0.5 in. diameter, 0.5 in. length, Master Magnetics, Marietta, OH) were mounted on a stepper-motor-driven translator, allowing them to be positioned from 120 mm to within 2 mm of the beads. Computer software (Labview, National Instruments, Austin, TX) measures vertical (*z*) bead position using a focusing algorithm, tracks transverse (*x*−*y*) motions of beads, and moves the magnets to change forces applied to the beads. Absolute vertical positions were determined using beads adsorbed to the cover glass.

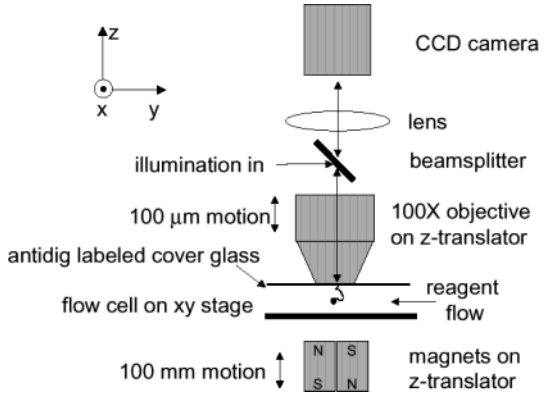

FIGURE 1: Experimental design. A 100× microscope objective on a piezoelectric focuser was used to visualize paramagnetic beads attached to the free end of a λ-DNA molecule tethered to a cover slip via an antibody linkage to the digoxygenin-labeled end. A "magnetic tweezer" consisting of a permanent magnet on a positioner mounted below the flow cell allowed controlled forces to be applied to the beads. Beads attached to the glass via single DNA molecules could be tracked in the vertical direction using the piezoelectric focuser; tracking in the *x*−*y* plane was done using images collected by a CCD camera.

Force Measurement, Calibration, and Single-Molecule Detection. Forces were measured using the fluctuation technique of Strick et al. (*27*, *28*). In short, following an extension (*z*) measurement, the computer acquires images and measures bead position in the *x*−*y* plane. Large fluctuations occur for low forces; progressively higher forces suppress the *x*−*y* fluctuations. For extensions greater than half the contour length, the relation between fluctuations and force is $f = 2k_BTz/\Delta^2$ (*27*) where $k_B = 1.38 \times 10^{-23}$ J/K is Boltzmann's constant (the gas constant divided by Avogadro's number), *T* is absolute temperature (298 K for all experiments), *z* is the average molecule extension along the force direction, and Δ^2 is the mean square displacement of the bead in the *x*−*y* plane. Thus measurement of extension (*z*) and *x*−*y* fluctuations (Δ^2) for one magnet position gives a calibrated force.

When a tether was first observed in buffer, a series of tests were done to check that it was a single DNA molecule. An initial test that a tether is a single DNA is of course its extension to a 16.5 μm length under high forces expected for 48.5 kb λ-DNA. Once this requirement was satisfied, extension and force measurements for five magnet positions were done. These data were used to determine the apparent

persistence length of the candidate molecule using the expected linear relation between $f^{-1/2}$ and extension, using the relation $z/L = 1 - (4Af/k_BT)^{-1/2}$ accurate for forces between 0.5 and 10 piconewtons (pN, or 10^{-12} N) (*29*). We expect a persistence length $A \sim 50$ nm for a single DNA; multiple DNAs will display lower apparent persistence lengths.

Once a tether with a force−extension relation matching that of naked DNA (*18*, *29*) was found, the calibration data are used to determine a force-versus-magnet position calibration, allowing us to know the force applied to a particular bead during the remainder of that experiment. After identification and calibration of a single-DNA tether, the PBS buffer was replaced with protein-binding buffer by flowing about 200 μL through the flow cell.

Protein−DNA Experiments. Two types of experiments were done. "Force−extension" experiments involved a series of measurements of tether extension at each of 20 forces (i.e., 20 magnet positions), ranging from 0.04 to 15 pN. The largest force obtained depends on the bead and can be as large as 20 pN. An "extension" series (increasing forces) was followed by a "retraction" series (decreasing forces), over a time of 6 min. Force−extension measurements were done first in protein-binding buffer (no protein); next we flowed 200 μL of buffer + protein through the sample; finally we remeasured the force−extension response of the same tether.

"Fixed force" experiments were done to study reaction kinetics. Extension measurements were made every 8 s at fixed magnet position corresponding to 0.5 pN, to give a time series of response of tethered DNA as the sample solution was changed. This allows direct observation of binding and unbinding kinetics, and tests of, e.g., chemical reversibility of reactions, under conditions where thermodynamic quantities, including force, were otherwise fixed.

RESULTS

Compaction of DNA by HMGB1 and NHP6A Increases with Increasing Protein Concentration. To evaluate DNA compaction by protein, single-DNA tethers were identified and a force−extension curve in protein-free binding buffer was recorded. Then, buffer plus protein was flowed into the sample cell and force−extension measurements were reobtained on the same molecule. Figure 2a shows results for experiments (different samples) with HMGB1. "Naked DNA" in binding buffer follows the expected force−extension curve for 16.3-μm-long λ-DNA (*18*). After flowing in 1 μM HMGB1, below 4 pN the HMGB1 + DNA is compacted relative to naked DNA. At lower forces compaction becomes progressively stronger, and as HMGB1 concentration is increased to 12 μM, extensions shift to progressively smaller values. In all cases studied, the HMGB1−DNA reaction was complete within 5 s of flow, and no hysteresis was observed during the 6 min extension−retraction scan.

Similar experiments were performed with NHP6A (Figure 2b). Compaction was observed for NHP6A beginning at 3 nM and increased with protein concentration up until 33 nM, at which point no further shift of the force−extension curve was detected.

The results for HMGB1 and NHP6A are qualitatively similar, with increasing compaction occurring at increasing

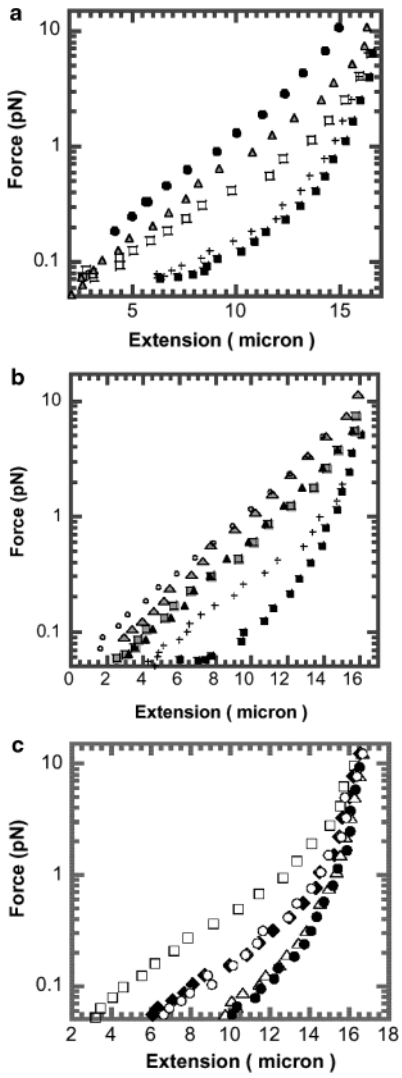

FIGURE 2: Single-molecule measurements of DNA compaction by HMGB1, NHP6A, and HU. Each data set represents an independent protein-binding experiment where naked DNA was reacted with one protein concentration. In each experiment, it was found that the force−extension curves measured during extension and during subsequent retraction were the same, i.e., that the mechanical response was reversible. (a) HMGB1. The force response of naked DNA (filled squares) was shifted to slightly higher forces after reaction with 1 μM HMGB1 (open squares). In separate experiments with higher HMGB1 concentrations of 3 μM (triangles) and 12 μM (filled circles) progressively stronger force shifts were observed. Following incubation of the 1 μM HMGB1−DNA complex in protein-free buffer the force−extension behavior was observed to return to that of naked DNA (crosses). (b) NHP6A. Force−extension curves again shifted to larger forces with progressively higher NHP6A concentration. Data are shown for naked DNA (filled squares), 3 nM (crosses), 5 nM (gray squares), 10 nM (filled triangles), and 33 nM (gray triangles), 75 nM (circles) NHP6A. NHP6A generated a larger force shift than HMGB1 at a given concentration; above 33 nM NHP6A this force-shift effect was saturated. (c) HU. The force−extension curve for naked DNA (filled diamonds) was shifted to higher forces by 100 nM HU (open squares); this effect was similar to that seen with NHP6A and HMGB1. However, for a larger HU concentration of 500 nM (open triangles), the force−extension curve shifted back to lower forces than for naked DNA. This indicates that 500 nM HU forms an HU−DNA structure which is stiffer than naked DNA. After incubation with 500 nM HU, a subsequent wash with buffer (see text) resulted in no shift of the force curve (filled circles); a further wash with buffer containing 0.1 mg/mL nonspecific DNA fragments returned the force−extension curve to that of naked DNA (open circles).

protein concentrations. However, the NHP6A−DNA interaction is considerably stronger since we observed a degree of compaction at concentrations of ~5 nM that is comparable to compaction by ~1 μM HMGB1. The magnitude of the difference in protein concentrations required to generate similar compaction forces corresponds to their difference in binding affinity to short DNA fragments, as measured under similar buffer conditions by PAGE mobility shift assays (data not shown and ref *4*). We were able to recover almost all of the initial 16.3 μm naked DNA length at high force (>10 pN), indicating that no DNA loops or sticking of DNA to the glass slide or surfaces occurred.

Binding of HU Exhibits a Bimodal Effect on DNA Elasticity. Similar experiments were performed with varying concentrations of *E. coli* HU protein (Figure 2c). At 100 nM HU, force−extension was shifted to larger forces relative to naked DNA indicating compaction in a manner resembling HMGB1 and NHP6A. At the higher concentration (500 nM) an "anticompaction" effect was revealed by a shift of the force−extension curve to smaller forces relative to naked DNA. In this new regime, lower forces were required to stretch out the HU−DNA complex; above 8 pN the HU−DNA complex force−extension response was close to that of naked DNA.

NHP6A Does Not Unbind from DNA into Protein-Free Buffer but Immediately Dissociates in the Presence of Excess Nonspecific DNA. To study protein binding and unbinding kinetics we measured DNA extension during changes in solution conditions. This is illustrated in Figure 3a, which shows a time course of DNA extension at a fixed force of 0.5 pN. Before addition of NHP6A, naked DNA showed the expected extension of 13.5 μm. Buffer containing 33 nM NHP6A was then injected (0 s); over the next *z*-measurement cycle (10 s) the molecule was compacted to a length of about 7 microns. After incubation with NHP6A (700 s), protein-free buffer was introduced, reducing the protein concentration in solution to zero. The compaction effect remained unchanged after 2400 s, indicating that NHP6A did not unbind from the DNA molecule. At the end of the time series (2400 s), buffer containing nonspecific DNA fragments (0.1 mg/mL, 300 bp DNA fragments, Promega, Madison, WI) was introduced. As the DNA fragments reached the molecule being observed, the DNA rapidly increased in molecule extension to its original length measured in protein-free buffer. Experiments with longer protein-free-buffer incubations showed that the protein remains stably bound to DNA on time scales of at least 3 h (data not shown).

To demonstrate that the stability of the DNA−protein complexes is force independent, force−extension curves of NHP6A−DNA were recorded after reaction with 10 nM NHP6A and subsequent washing with protein-free buffer (Figure 3b). Forces of up to 8 pN did not promote any change in the force−extension curve, and therefore no dissociation of protein, in either protein solution or protein-free buffer.

Finally, buffer containing nonspecific DNA was introduced. The resulting curve is identical to the naked DNA curve, indicating that the competitor DNA released the protein bound to the DNA that we were observing. The absence of NHP6A dissociation into protein-free buffer, followed by apparently complete transfer of protein to nonspecific DNA, occurred in experiments using NHP6A at concentrations from 3 nM to 75 nM.

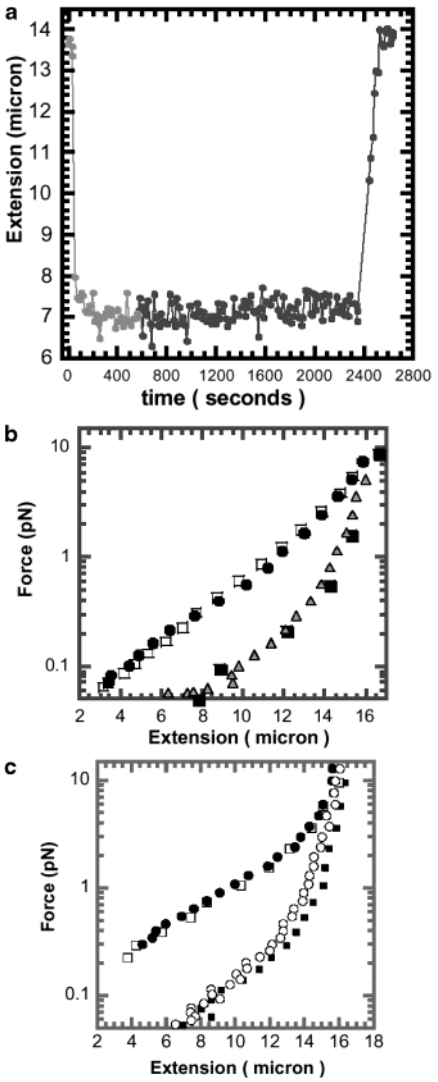

FIGURE 3: Binding and unbinding of NHP6A and HMGB1. (a) Time course experiment with NHP6A at a constant force of 0.5 pN. The naked DNA extension of 13.5 μm (0 s) was rapidly reduced to 7 μm when buffer containing 33 nM NHP6A was flowed into the sample. Protein-free buffer was then flowed past the NHP6A−DNA complex (at 700 s); no return of the extension toward the initial value was observed in protein-free buffer (from 700 s to 2400 s). Finally, buffer containing nonspecific DNA fragments (0.1 mg/mL) was flowed into the sample (at 2400 s); this caused a rapid return of the extension to its original naked-DNA value. (b) High stability of DNA−NHP6A complex. First, naked DNA in protein-free buffer (filled squares) was measured. Next, 10 nM NHP6A (open squares) led to a shift to higher forces. Subsequently, the sample was washed with protein-free buffer; the resulting force−extension curve (filled circles) is unchanged from the 10 nM protein curve. Finally, a wash with buffer containing nonspecific DNA fragments resulted in a return of the force−extension curve to its prebound DNA shape (triangles). (c) High stability of DNA−HMGB1 complex. The naked DNA force response (filled squares) was shifted to larger forces by 2 μM HMGB1 (open squares). A subsequent wash by protein-free buffer did not change the force curve (filled circles). Finally, a wash with nonspecific DNA fragments resulted in a return of the force response to its prebound DNA shape (open circles).

HMGB1 Binding−Unbinding Kinetics Is Concentration Dependent. Similar binding−unbinding experiments were performed with HMGB1. Figure 2a shows the effect of a protein-free buffer wash after binding and compaction by 1 μM HMGB1. The force curve returned to near that of naked DNA, indicating that 1 μM HMBG1 binds to DNA in a

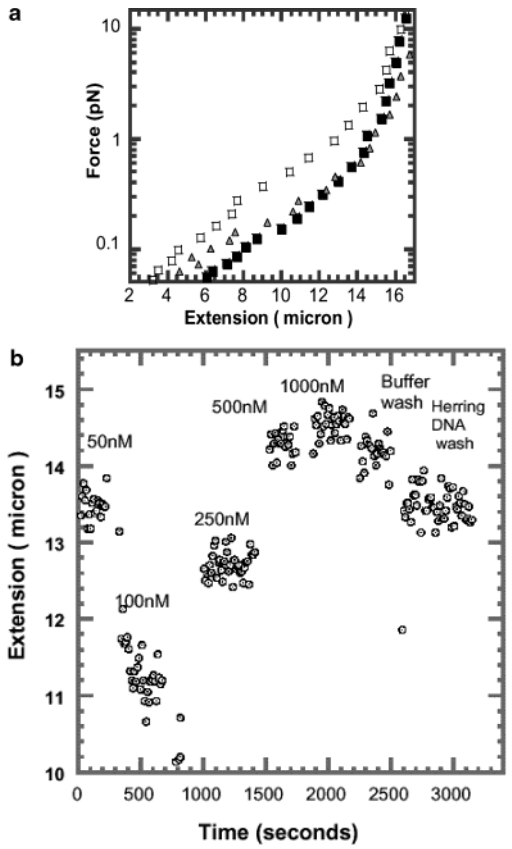

FIGURE 4: Spontaneous unbinding of HU in the DNA compaction regime (a) and stable binding in the DNA stiffening regime (b). (a) Force curves of naked DNA (filled squares) and DNA after compaction by 100 nM HU (open squares). When the tethered DNA was then washed with protein-free buffer, its force−extension response returned to that of naked DNA (triangles). (b) A constant force of 0.5 pN was used during a series of solution changes. Naked DNA in protein-free buffer (0 s) and 50 nM HU (250 s) showed the same length of 13.5 μm. Flow of 100 nM HU (500 s) compacted the DNA to about 11 μm in length. Then, flow of 250 nM HU (1000 s) decompacted DNA, causing the extension to increase to about 13 μm. Subsequent reactions with 500 nM (1600 s) and 1 μM HU (2000 s) increased DNA extension to larger than the naked DNA value. A wash with protein-free buffer (2400 s) caused only a small reduction in DNA extension, indicating that HU remained bound. However, a wash with buffer containing 0.1 mg/mL nonspecific DNA fragments (2700 s) led to a return of the DNA extension to its prebound value.

manner allowing spontaneous unbinding into protein-free solution.

In the experiment illustrated in Figure 3c, protein-free buffer was introduced after the DNA was compacted by incubation with 2 μM HMGB1. No change in force−extension response was observed after the wash with protein-free buffer. Introduction of nonspecific DNA fragments into the solution caused the force−extension curve to return to that of the original, naked DNA. Thus, HMGB1 does not spontaneously dissociate into protein-free solution after binding at HMGB1 concentrations from 2 μM to 12 μM (Figure 3c and data not shown), but it will rapidly unbind from DNA in the presence of nonspecific DNA fragments.

HU Binding−Unbinding Kinetics Are Concentration Dependent. HU exhibited concentration-dependent differences in binding kinetics that correlated with its mode of DNA compaction. Figure 4a shows a binding-dissociation experiment performed at intermediate HU concentrations (100 nM) where HU compacts DNA. When protein-free solution was then flowed into the sample, the force−extension curve returned back to that of naked DNA (triangles). Thus, binding of HU at intermediate concentrations where DNA compaction occurs is reversible.

On the other hand, HU bound at higher concentrations, where it increases DNA rigidity, no longer dissociates into solution. Figure 2c shows the stiffening of DNA induced by HU at 500 nM. At this concentration, the force−extension curve remains unchanged by washing with protein-free buffer, indicating that HU is not dissociating from the tethered DNA. However, a switch to buffer containing nonspecific DNA resulted in the mechanical properties of the DNA returning to that of the naked molecule, as observed for the HMGB proteins.

An HU Titration Series on a Single Molecule at a Fixed Force Demonstrates Compaction, Stiffening, and DNA-Dependent Dissociation. Figure 4b shows DNA extensions at a fixed force of 0.5 pN, for a series of solutions with different concentrations of HU. DNA with 50 nM HU was observed to have about the same length as naked DNA (~13.5 μm). Addition of 100 nM HU decreased the length of the DNA molecule to 11 μm. The DNA length then increased as higher concentrations of HU were added such that 500 nM and 1 μM HU resulted in lengths greater than that of naked DNA. After reaction with 1 μM HU, the DNA was washed with protein-free buffer. The DNA extension only slightly shifted toward that of naked DNA, indicating that a significant portion of the bound protein remained on the DNA. However, this remaining protein was rapidly removed by addition of nonspecific DNA fragments, as shown by the return of the extension to that of naked DNA.

DISCUSSION

We have studied DNA compaction by two classes of nonspecific DNA-bending proteins using single-DNA micromanipulation. For two different HMGB−DNA complexes (NHP6A and HMGB1), increasing protein concentrations required progressively greater mechanical forces to stretch the DNA to its prebound length. The absolute protein concentrations that generated equivalent compaction forces correspond well to their known relative DNA binding affinities, with yeast NHP6A inducing compaction forces that were equivalent to those observed with mammalian HMGB1 at substantially lower protein concentrations.

E. coli HU protein exhibited bimodal behavior as a function of protein concentration. At intermediate protein concentrations, HU compacted DNA comparably to the two HMGB proteins. Remarkably, at higher concentrations, HU caused DNA to stiffen, as reflected by the reduction of mechanical forces required to stretch the double helix.

The micromechanics of HMGB protein−DNA complexes over a broad range of concentrations and HU at intermediate concentrations is in accord with theoretical expectations for DNA-bending proteins (*22*), in that as increasing amounts of these proteins are bound, the number of bends induced in the DNA is increased. Effectively, this causes a decrease of DNA persistence length, resulting in progressive DNA compaction. Theoretical modeling has shown that when the distance between protein-induced bends becomes less than about two persistence lengths (the distance over which

thermal forces generate appreciable DNA bending, about 300 bp) the force needed to half-extend a DNA should be nearly doubled (*22*).

For example, in Figure 2a, the naked DNA curve shows that 10 μm extension occurs for about 0.1 pN of force. For 1 μM HMGB1, a 0.2 pN force is required for the same 10 μm extension. This change in mechanical response indicates that, at 1 μM protein concentration, one HMGB1 is bound per 300 bp of DNA. Our sensitivity to this relatively sparse occupation of DNA by protein is due to B-DNA's stiffness: a DNA-bending protein perturbs DNA conformation over a long ($\sim$50 nm) distance. Further quantitative analysis will require independent measurement of protein coverage, possibly via quantitative fluorescence.

Unbinding of HMGB1−, NHP6A−, and HU−DNA Complexes into Solution. The use of tethered DNA molecules allows mechanical properties of a molecule to be followed in real time, during changes in solution conditions. Remarkably, we found that the force−extension curves did not generally return to their "naked DNA" shape when protein was removed from solution. Indeed, NHP6A did not dissociate from tethered DNA into protein-free buffer following binding at any protein concentration where a compaction effect was detected. For HMGB1, spontaneous protein dissociation into protein-free buffer occurred from DNA complexes assembled under protein concentrations (1 μM) where moderate compaction was generated. However, following binding using 2 μM to 12 μM HMGB1, DNA compaction remained unchanged after washing with protein-free buffer for several hours. Thus, the off-time into protein-free buffer of HMGB1−DNA complexes assembled above a concentration threshold of roughly 2 μM is well in excess of 1000 times the apparent few-second-long binding reaction.

The stability of HU−DNA complexes also varied dramatically as a function of initial binding concentration. HU readily dissociated into protein-free solution when bound at an initial concentration of 100 nM where it compacts DNA. However, at initial binding concentrations at or above 0.5 μM, where it increases the rigidity of DNA, HU failed to dissociate into protein-free solution.

In all cases where protein-induced compaction was observed, we found that forces of up to 15 pN do not induce dissociation of NHP6A, HMGB1, or HU from DNA, even though these forces were sufficient to extend the protein−DNA complexes to a length nearly equal to that of the bare DNA. This indicates that the protein−DNA complexes are flexible; the bending may be eliminated by force, while the proteins remain bound. For HU, this observation is consistent with previous structural studies (*14*) and with recent results of van Noort et al. (*24*). Our experiments with HMGB1 and NHP6A indicate that these proteins also form flexibly bent DNA−protein complexes.

HMGB1, NHP6A, and HU Can Readily Dissociate from DNA via Direct Transfer to a Different DNA Segment, Even When Dissociation into Solution Cannot Occur. Although HMGB1−DNA, NHP6A−DNA, and HU−DNA complexes were stable in protein-free solution, the proteins rapidly dissociated from the tethered DNA when DNA fragments were flowed into the sample. Thus, our results indicate that while there is a large barrier to removal of these proteins from DNA into solution, there apparently exists little or no barrier to their transfer onto a nearby DNA fragment. This "direct transfer" mechanism for moving protein between DNA segments may be important for shifting proteins between DNA sites in vivo, where DNA concentrations are high and DNA−DNA collisions are frequent.

The Bimodal Effect of HU on DNA Elasticity. We can estimate effects of different HU concentrations on apparent persistence length of DNA by fitting the force−extension curves to the wormlike chain model (*29*). For extensions of 10 to 16 μm, extension data of Figure 2c fit well to the form $z = L - (k_B T/4Af)^{1/2}$, where k_B is Boltzmann's constant, $T = 300$ K is room temperature, L is the molecule length of 16.5 μm, and A is the persistence length. For the naked and nonspecific-DNA-washed data we obtain $A = 43$ nm, close to the expected $\sim$50 nm (*18*). At 100 nM HU, bending-induced compaction reduces apparent persistence length to 13 nm, but at 500 nM HU, the apparent persistence length is increased to 103 nm.

Our observation of an increase in persistence length by high concentrations of HU is consistent with recent SFM imaging (*9*). For high HU/DNA ratios (1 HU dimer per 9 bp of DNA), Dame and Goosen found that the DNA molecules adopted a straighter appearance with slight extension of their average contour length. In vitro binding studies employing native gel electrophoresis to quantify the number of complexes formed with increasing amounts of HU on short DNA fragments have indicated that HU can effectively coat the DNA. At saturating concentrations, HU dimers bind at stoichiometries of up to 1 HU dimer per 9 bp (*30*). Moreover, nuclease digestion products obtained at high HU−DNA concentrations have been found to exhibit an 8.5−9 bp periodicity (*31*). Finally, we note that van Noort et al. have also recently reported (*24*) single-DNA experiments showing the same bimodal compaction−stiffening effects discussed in this paper. Our two sets of experiments are in excellent agreement; in addition new SFM results of van Noort et al. suggest that, in its stiffening mode, HU binds onto DNA so as to form a fiber with a regular helical structure (*24*). Recent FRET data of Sagi et al. (*32*) are also consistent with this HU-concentration-dependent bimodal binding picture.

Recent crystal structures of HU bound to DNA may provide insight into the mechanism responsible for DNA stiffening at high binding densities (*12*). Within the cocrystals, individual HU−DNA complexes align to form pseudo-continuous DNA helices that adopt extended, but serpentine-like structures. The HU−DNA interface predominantly consists of the two β-ribbon arms emanating from each subunit of the dimer in opposite directions along the DNA minor groove. Although prolines at the ends of the arms induce kinks into the DNA by inserting into the base stack, the 9 bp intervening DNA segment is essentially straight. In one crystal form, HU contacts with DNA are limited to as few as 14 bp. Molecular modeling suggests that HU dimers could potentially assemble onto a DNA polymer with an even closer spacing between adjacent dimers, which could effectively lead to an even more extended DNA helix than observed in the crystals (*12*). At lower HU to DNA ratios the DNA flanking the sites of proline insertion is predicted to dynamically associate with the basic sides of the HU dimer in a manner analogous to the path of DNA within the IHF cocrystal structure where the DNA is bent nearly 180° (see Swinger et al. (*12*)). In this wrapping mode, DNA molecules could adopt either highly compact serpentine or toroidal

structures depending upon the spacing and helical phasing of the bends.

HU is present throughout the nucleoid in exponentially growing bacterial cells at an average level of about one dimer per several hundred base pairs (*7*, *33*−*36*). Our force−extension data at intermediate HU concentrations indicates that HU binding at physiological levels will significantly contribute to chromosome compaction. However, if high local HU concentrations are achieved in vivo, the stabilized-stiffening mode of binding will occur.

Consistent with an important role of HU in chromosome compaction, *hupAB* mutants lacking both subunits of HU display decondensed nucleoids and reduced superhelical densities (*4*, *15*−*17*). Moreover, in many of the specialized roles that HU performs in vivo, one or a small number of HU dimers are clearly functioning by inducing DNA bends. For example, HU promotes loop formation between operator sites to enhance transcriptional repression by GalR and between enhancer and recombination sites to facilitate invertasome formation in the Hin recombination system (*37*, *38*). Stiffening of DNA by HU in these systems would be counterproductive.

What Mechanism Drives Formation of Stable Complexes by HMGB1, NHP6A, and HU? Once formed, the highly stable protein−DNA complexes reported in this paper face a large free energy barrier for their removal, since we observe no protein dissociation to protein-free solution on time scales thousands of times larger than the apparent on-time. Intriguingly, we have observed these stabilized complexes for HMGB and HU proteins, which are not related, apart from their function as nonspecific DNA-bending proteins.

An important clue to the mechanism stabilizing these proteins on DNA comes from the cases of HMGB1 and HU, where two regimes of protein−DNA binding can be observed. At lower concentrations, there is a "reversible binding" regime where the protein will dissociate to protein-free buffer. Then, at higher concentrations, there is an "irreversible binding" regime where the protein will no longer leave the DNA when protein-free buffer is introduced. Therefore, for HMGB1 and HU, the stability of the protein−DNA complexes formed depends on the solution protein concentration during binding. In the case of NHP6A, binding always occurs so as to form highly stable complexes.

The above results indicate that after the protein concentration threshold for stabilized binding is reached, the proteins HMGB1, NHP6A, and HU are no longer binding in a simple, independent (i.e., two-state, or on/off) manner. If the proteins had bound (and by detailed balance, unbound) independently of one another, we should have expected a return to the bare DNA response when protein-free buffer was introduced. Additionally, the time scale we would expect for dissociation to protein-free buffer should be comparable to the binding time near the apparent association concentrations (roughly 3 nM for NHP6A, 1 μM for HMGB1, 100 nM for HU; recall that, for independent binding, the on- and off-times should be equal at the association point). Instead, we observe that when these proteins are bound above the stabilization concentration, the off-time is at least a few thousand times longer than the on-times. This asymmetry rules out the possibility that we can consider binding of individual proteins in an independent fashion once stabilized complexes are forming.

A possible explanation for the protein-concentration-dependent stability is cooperativity of the protein−DNA interaction. Cooperative binding by HMGB and HU proteins has been implicated in other experiments. Two protomers of HMGB1, NHP6A, or HU bind to DNA microcircles in a strongly cooperative fashion (*26*, *39*) (B.W. and R.C.J., unpublished). Isothermal titration calorimetry experiments have provided evidence of HMGB1 cooperatively binding to poly-dAT, but interestingly not to poly-dGC, linear duplexes (*40*). A recent study probing HU-induced DNA bending by FRET argued that HU cooperatively binds to 55 bp DNAs (*32*), but another study that also examined DNA bending concluded that two molecules of HU bound in a independent, stepwise manner to a 29 bp region (*41*).

Available structural data do not indicate obvious sites of protein−protein interaction, although a direct protein−protein contact mechanism cannot be ruled out. Furthermore, HMGB1, NHP6A, and HU do not exhibit signs of strong interactions by themselves; they are highly soluble, and do not aggregate or polymerize in concentrated solution. We do not find strong dependence of the stabilization we have observed on salt concentration: experiments on HMGB1 and NHP6A in 150 mM NaCl buffer, and also in the presence of 1 to 5 mM of Mg^{2+} (data not shown), show the same strong stability after binding as reported for 40 mM NaCl in this paper. Thus, there is not strong evidence suggesting cooperativity via protein−protein interactions

An alternate mechanism for cooperativity could be based on distortion of the underlying DNA. We speculate that binding of one protein might, by distorting DNA near the binding site, make adjacent binding of a second protein favorable. Since DNA strand separation is itself highly cooperative, disruption of DNA secondary structure, through severe local bending or twisting, could play a role in driving adjacent binding of "architectural" DNA proteins so as to form organized nucleoprotein structures. For the DNA-bending proteins studied here, the role of helix-opening cooperativity is not clear since they induce only local disruptions of DNA secondary structure. However, it has been observed that distorted DNA structures are favored HMGB and HU protein binding sites (*1*, *3*, *14*, *42*), and it would be of interest to carry out experiments along the lines of those presented here to study how distorted DNA substrates affect binding stability.

ACKNOWLEDGMENT

We are grateful to D. Chatenay, P. Rice, B. Schnurr, and J. Stavans for helpful discussions, and to R. T. Dame for communication of ref *24* prior to its publication. We also thank A. Nemani and Y. Pan for their help with construction of the apparatus.

REFERENCES

1. Bustin, M. (1999) Regulation of DNA-dependent activities by the functional motifs of the high-mobility-group chromosomal proteins, *Mol. Cell. Biol. 19*, 5237−46.
2. Bianchi, M. E., and Beltrame, M. (2000) Upwardly mobile proteins. Workshop: the role of HMG proteins in chromatin structure, gene expression and neoplasia, *EMBO Rep. 1*, 109−14.
3. Thomas, J. O., and Travers, A. A. (2001) HMG1 and 2, and related 'architectural' DNA-binding proteins, *Trends Biochem. Sci. 26*, 167−74.

4. Paull, T. T., and Johnson, R. C. (1995) DNA looping by *Saccharomyces cerevisiae* high mobility group proteins NHP6A/B. Consequences for nucleoprotein complex assembly and chromatin condensation, *J. Biol. Chem. 270*, 8744−54.
5. Megraw, T. L., and Chae, C. B. (1993) Functional complementarity between the HMG1-like yeast mitochondrial histone HM and the bacterial histone-like protein HU, *J. Biol. Chem. 268*, 12758−63.
6. Johnson, R. C., Johnson, L. M., Schmidt, J. W., and Gardner, J. F. (2004) in *The Bacterial Chromosome* (Higgins, N. P., Ed.) in press, ASM Press, Washington, D.C.
7. Drlica, K., and Rouviere-Yaniv, J. (1987) Histone-like proteins of bacteria, *Microbiol. Rev. 51*, 301−19.
8. Nash, H. A. (1996) in *Regulation of Gene Expression in Escherichia coli* (Lin, E. E. C., and Lynch, A. S., Eds.) pp 149−79, R. G. Landes Co., Austin, TX.
9. Dame, R. T., and Goosen, N. (2002) HU: promoting or counteracting DNA compaction? *FEBS Lett. 529*, 151−6.
10. Lavoie, B. D., Shaw, G. S., Millner, A., and Chaconas, G. (1996) Anatomy of a flexer-DNA complex inside a higher-order transposition intermediate, *Cell 85*, 761−71.
11. Kamashev, D., Balandina, A., and Rouviere-Yaniv, J. (1999) The binding motif recognized by HU on both nicked and cruciform DNA, *EMBO J. 18*, 5434−44.
12. Swinger, K. K., Lemberg, K. M., Zhang, Y., and Rice, P. A. (2003) Flexible DNA bending in HU-DNA cocrystal structures, *EMBO J. 22*, 3749−60.
13. Wojtuszewski, K., and Mukerji, I. (2003) HU binding to bent DNA: a fluorescence resonance energy transfer and anisotropy study, *Biochemistry 42*, 3096−104.
14. Swinger, K. K., and Rice, P. A. (2004) IHF and HU: flexible architects of bent DNA, *Curr. Opin. Struct. Biol. 14*, 28−35.
15. Dri, A.-M., Rouviere-Yaniv, J., and Moreau, P. L. (1991) Inhibition of cell division in *hupA hupB* mutant bacteria lacking HU protein, *J. Bacteriol. 173*, 2852−63.
16. Huisman, O., Faelen, M., Girard, D., Jaffe, A., Toussaint, A., and Rouviere-Yaniv, J. (1989) Multiple Defects in *Escherichia coli* mutants lacking HU protein, *J. Bacteriol. 171*, 3704−12.
17. Hillyard, D. R., Edlund, M., Hughes, K. T., Marsh, M., and Higgins, N. P. (1990) Subunit-specific phenotypes of *Salmonella typhimurium* HU mutants, *J. Bacteriol. 172*, 5402−7.
18. Bustamante, C., Smith, S. B., Liphardt, J., and Smith, D. (2000) Single-molecule studies of DNA mechanics, *Curr. Opin. Struct. Biol. 10*, 279−85.
19. Finzi, L., and Dunlap, D. (2003) Single-molecule studies of DNA architectural changes induced by regulatory proteins, *Methods Enzymol. 370*, 369−378.
20. Ali, B. M., Amit, R., Braslavsky, I., Oppenheim, A. B., Gileadi, O., and Stavans, J. (2001) Compaction of single DNA molecules induced by binding of integration host factor (IHF), *Proc. Natl. Acad. Sci. U.S.A. 98*, 10658−63.
21. Marko, J. F., and Siggia, E. D. (1997) Driving proteins off DNA using applied tension, *Biophys. J. 73*, 2173−8.
22. Yan, J., and Marko, J. F. (2003) Effects of DNA-distorting proteins on DNA elastic response, *Phys. Rev. E 68*, 011905.
23. Cocco, S., Marko, J. F., Monasson, R., Sarkar, A., and Yan, J. (2003) Force-extension behavior of folding polymers, *Eur. Phys. J. E 10*, 249−63.
24. van Noort, J., Verbrugge, S., Goosen, N., Dekker, C., Dame, R. T. (2004) Dual architectural roles of HU: Formation of flexible hinges and rigid filaments, *Proc. Natl. Acad. Sci. U.S.A. 101*, 6969−74.
25. Paull, T. T., Haykinson, M. J., and Johnson, R. C. (1993) The nonspecific DNA-binding and -bending proteins HMG1 and HMG2 promote the assembly of complex nucleoprotein structures, *Genes Dev. 7*, 1521−34.
26. Yen, Y. M., Wong, B., and Johnson, R. C. (1998) Determinants of DNA binding and bending by the Saccharomyces cerevisiae high mobility group protein NHP6A that are important for its biological activities. Role of the unique N terminus and putative intercalating methionine, *J. Biol. Chem. 273*, 4424−35.
27. Strick, T. R., Allemand, J. F., Bensimon, D., Bensimon, A., and Croquette, V. (1996) The elasticity of a single supercoiled DNA molecule, *Science 271*, 1835−7.
28. Strick, T. R., Allemand, J. F., Bensimon, D., and Croquette, V. (1998) Behavior of supercoiled DNA, *Biophys. J. 74*, 2016−28.
29. Marko, J. F., and Siggia, E. D. (1995) Stretching DNA, *Macromolecules 28*, 8759−70.
30. Bonnefoy, E., and Rouviere-Yaniv, J. (1991) HU and IHF, two homologous histone-like proteins of Escherichia coli, form different protein-DNA complexes with short DNA fragments, *EMBO J. 10*, 687−96.
31. Broyles, S. S., and Pettijohn, D. E. (1986) Interaction of the *Escherichia coli* HU protein with DNA: evidence for formation of nucleosome-like structures with altered DNA helical pitch, *J. Mol. Biol. 187*, 47−60.
32. Sagi, D., Friedman, N., Vorgias, C., Oppenheim, A. B., and Stavans, J. (2004) Modulation of DNA conformations through the formation of alternative high-order HU-DNA complexes, *J. Mol. Biol. 341*, 419−28.
33. Shellman, V. L., and Pettijohn, D. E. (1991) Introduction of proteins into living bacterial cells: distribution of labeled HU protein in *Escherichia coli*, *J. Bacteriol. 173*, 3047−59.
34. Ali Azam, T., Iwata, A., Nishimura, A., Ueda, S., and Ishihama, A. (1999) Growth phase-dependent variation in protein composition of the *Escherichia coli* nucleoid, *J. Bacteriol. 181*, 6361−70.
35. Wery, M., Woldringh, C. L., and Rouviere-Yaniv, J. (2001) HU-GFP and DAPI co-localize on the *Escherichia coli* nucleoid, *Biochimie 83*, 193−200.
36. Azam, T. A., Hiraga, S., and Ishihama, A. (2000) Two types of localization of the DNA-binding proteins within the *Escherichia coli* nucleoid, *Genes Cells 5*, 613−26.
37. Haykinson, M. J., and Johnson, R. C. (1993) DNA looping and the helical repeat in vitro and in vivo: effect of HU protein and enhancer location on Hin invertasome assembly, *EMBO J. 12*, 2503−12.
38. Lewis, D. E., Geanacopoulos, M., and Adhya, S. (1999) Role of HU and DNA supercoiling in transcription repression: specialized nucleoprotein repression complex at gal promoters in *Escherichia coli*, *Mol. Microbiol. 31*, 451−61.
39. Webb, M., Payet, D., Lee, K. B., Travers, A. A., and Thomas, J. O. (2001) Structural requirements for cooperative binding of HMG1 to DNA minicircles, *J. Mol. Biol. 309*, 79−88.
40. Muller, S., Bianchi, M. E., and Knapp, S. (2001) Thermodynamics of HMGB1 interaction with duplex DNA, *Biochemistry 40*, 10254−61.
41. Arthanari, H., Wojuszewski, K., Mukerji, I., Bolton, P. H. (2004) Effects of HU binding on the equilibrium cyclization of mismatched, curved, and normal DNA, *Biophys. J. 86*, 1625−31.
42. Travers, A. (2000) Recognition of distorted DNA structures by HMG domains, *Curr. Opin. Struct. Biol. 10*, 102−9.

BI048428O